A Ground Validation Network for the Global Precipitation Measurement Mission

Mathew R. Schwaller and K. Robert Morris
Global Precipitation Mission Project
NASA/Goddard Space Flight Center
Greenbelt, Maryland USA 20771

Date of receipt: ____________________

Corresponding author's address:
Mathew R. Schwaller
Global Precipitation Mission Project
NASA/Goddard Space Flight Center
Mail Codes 422 & 587
Greenbelt, Maryland USA 20771

mathew.r.schwaller@nasa.gov
phone: 301-614-5382
fax: 301-286-1787

A Ground Validation Network for the Global Precipitation Measurement Mission

Abstract

A prototype Validation Network (VN) is currently operating as part of the Ground Validation System for NASA's Global Precipitation Measurement (GPM) mission. The VN supports precipitation retrieval algorithm development in the GPM pre-launch era. Post-launch, the VN will be used to validate GPM spacecraft instrument measurements and retrieved precipitation data products.

The period of record for the VN prototype starts on August 8, 2006 and runs to the present. The VN database includes spacecraft data from the TRMM Precipitation Radar (PR) and coincident ground radar (GR) data from operational meteorological networks in the U.S., Australia, Korea, and the Kwajalein Atoll in the Marshall Islands. Satellite and ground radar data products are collected whenever the PR satellite track crosses within 200 km of a VN ground radar, and these data are stored permanently in the VN database. VN products are generated from coincident PR and GR observations when a significant rain event occurs.

The VN algorithm matches PR and GR radar data (including retrieved precipitation data in the case of the PR) by calculating PR and GR averages at the geometric intersection of the PR rays with the individual GR radar elevation sweeps. The algorithm thus averages the minimum PR and GR sample volumes needed to "match-up" spatially coincident PR and GR data types. The result of this technique is a set of vertical profiles for a given rainfall event, with coincident PR and GR samples matched at specified heights throughout the profile.

VN data can be used to validate satellite measurements and to track ground radar calibration over time. A comparison of matched TRMM PR and GR radar reflectivity factor data found a remarkably small difference between the two when averaged over the period of record of the VN data set.

1. Introduction

In collaboration with its international partners, NASA is developing a Ground Validation System (GVS) as a contribution to the Global Precipitation Measurement (GPM) mission. In the U.S., GPM has been recognized as a key weather and climate mission for providing uniform, global precipitation products that leverage all available satellites capable of precipitation measurement (NAS 2007). In achieving these goals, GPM addresses the call for "essential climate variables" as defined by the Global Climate Observing System (GCOS 2004). The GPM framework is also intended to be a realization of a "precipitation constellation" of satellites and ground-based assets that will deliver fundamental climate data records for social benefit (Neeck and Oki 2007).

The international GPM mission extends observations of the Tropical Rainfall Measuring Mission (TRMM, Simpson et al 1996) to precipitation at higher latitudes, with more frequent sampling, and with research focused on a more complete understanding of the global hydrological cycle. GPM will be capable of measuring rain rates as small as a hundredth of an inch per hour to as large as 4 inches an hour. GPM products will estimate the various sizes of precipitation particles, and will also discriminate between snow and rain. Mission requirements specify that precipitation products will be available with a 3-hour average revisit time over 80% of the globe, and data will be available to users within 3 hours of observation (Hou et al. 2008).

In support of the international GPM, NASA is planning to launch a GPM Core Satellite into a medium (65°) inclination orbit no later than July 2013. Current plans call for the GPM Ground Validation System (GVS) to support the GPM satellite mission. In the pre-launch era, the GPM GVS provides data to support the development of precipitation retrieval algorithms. In the post-launch era, the GPM GVS provides an independent means for evaluation, diagnosis, and ultimately improvement of GPM space-borne measurements and precipitation products.

This paper specifically describes one component of the GPM GVS: a Validation Network (VN) that compares GPM Dual-frequency Precipitation Radar (DPR) data products to similar measurements and products from national networks of operational weather radars and precipitation gauges. The goal for such comparisons is to understand and resolve the first order variability and bias of precipitation retrievals in different meteorological and hydrological regimes at large scales. Although the VN is intended for GPM validation, an initial version of the system is now in operation that uses TRMM satellite data. The current version of the VN is built on methods, research results, and computer code described by Anagnostou et al. (2000), Bolen and Chandrasekar (2000), Liao et al. (2001), and Bolen and Chandrasekar (2003).

As part of the international GPM mission, the VN is designed to incorporate and exploit data contributed by an arbitrary number of national meteorological networks of ground radars and precipitation gauges. At present, the VN includes contributions from ground radars located in Australia, South Korea, Kwajalein atoll in the Marshall Islands, and the southeastern U.S. But the system, as described below, was designed to be readily scalable. Thus, the VN allows for inclusion of new radars and additional national networks with only minor modification to VN code and database tables. Future plans call for the inclusion of spacecraft microwave radiometer data into the VN.

2. VN data sources

The current period of record for the VN data starts on August 8, 2006 and runs to the present. The current VN database includes spacecraft data from the TRMM Precipitation Radar (PR) and coincident ground radar (GR) data from several sources as described below. Satellite and ground radar data products are collected whenever the PR satellite track crosses within 200 km of a VN ground radar, and these data are stored permanently in the VN database. The generation of VN products from the coincident PR and GR data sets, however, occurs only when there is a "significant rain event," as defined in Section 3. Because many of the ground radar datasets are quality controlled by a human analyst prior to ingest into the VN, there is a variable time lag between observation and VN product creation.

TRMM PR. PR data are extracted from standard TRMM Version 6 data products 1C-21, 2A-23, 2A-25, and 2B-31 for orbital overpass events where the instrument ground track coincides with a VN ground radar. The extracted PR data include radar reflectivity (both raw and attenuation corrected), near-surface rain rate, and other variables (see Section 4). The VN acquires these data as orbit subset products directly from NASA's Precipitation Processing System (PPS, http://pps.gsfc.nasa.gov/pps). The PR data, along with detailed product descriptions, are also available to the public via NASA's Goddard Earth Sciences Data and Information Services Center (GES DISC, http://disc.sci.gsfc.nasa.gov).

At the current TRMM orbital altitude of 402 km, the 13.8 GHz (Ku band) PR data are characterized by a ground-level instantaneous field of view of approximately 5 km. The instrument scans along the satellite cross-track direction to yield a 247 km swath, with 49 ray samples in each cross-track scan. Within each ray, the PR samples a column of the atmosphere in series of range bins, each with a vertical resolution of 250 m, from ground level up to 20 km (Kozu et al. 2001).

WSR-88D. At present, the VN acquires ground radar data for 21 of the 59 NOAA- and DoD-owned Weather Service Radar-88D (NEXRAD) radar sites in the continental U.S. that are within view of the PR instrument. This 21 site subset falls within a bounding area with latitudes below 33°N and longitudes east of 98°W, plus KHTX at 34.9°N and 86.1°W (see Figure 1 and Table 1). Raw data are acquired from the WSR-88D Level II archive. In addition, the VN acquires WSR-88D data for these sites that have been quality-controlled via the methods applied to the TRMM standard product 1C-51. The 1C-51 algorithm includes screening by automated methods and by an analyst to remove non-meteorological radar echoes such as clutter associated with insects, birds, chaff, wildfires, antenna towers, and anomalous propagation (Rosenfeld et al. 1995). Data ingested from these sources include radar reflectivity factor, near-surface rainfall, and derived variables.

The WSR-88D radars operate at S-band (2.7-3.0 Ghz), and scan using a variety of weather-dependent standard volume coverage patterns. Data are collected as 360° full scans at a varying number of elevation angles from 0.5° to 19.5°, with gaps between the upper elevation sweeps. The WSR-88D products used in the VN provide sample volumes with a range resolution of 1 km and an azimuth resolution of 1°. The typical WSR-88D precipitation mode volume scan repeats every 4-6 minutes (NOAA 2006).

Gosan Radar. Data from the Gosan radar are provided to the VN by the National Institute of Meteorological Research (METRI) of the Korea Meteorological Administration (KMA). KMA operates a total of 12 C-band and S-band radars within South Korea. These, together with radars operated by the Korean Air Force and the U.S. Air Force constitute an operational network of 18 radars covering the whole of the southern Korean Peninsula. At present, data from a single South Korean radar at Gosan have been ingested into the VN. The Gosan radar (RSGN) is an S-band (4 GHz) radar operating with a range resolution of 0.125 km and an azimuth resolution of about 1°, and a nominal range of 250 km. The Gosan radar carries out one volume scan at 10 to 15 elevation angles from 0° to 45° every 10 minutes (Park and Lee, 2007).

ARMOR radar. The Advanced Radar for Meteorological and Operational Research (ARMOR) is a scanning dual-polarimetric Doppler radar operating at C-band (5625 MHz) with a beam width of 1°. It was originally deployed in Huntsville by the National Weather Service as a local warning radar in 1977 (WSR-74C), refurbished and upgraded to Doppler in 1991. The radar was donated to the University of Alabama, Huntsville Department of Atmospheric Science in 2002, and upgraded to dual-polarimetry using the SIGMET Antenna Mounted Receiver in Fall 2004 (Petersen et al. 2007).

Darwin radar. The Australian Bureau of Meteorology (BOM) operates the Darwin (DARW) CPOL radar (Keenan et al., 1998), which is a C-band (5625 MHz) scanning radar with a beam width of 1° and polarimetric capability.

Kwajalein radar. The Kwajalein radar (KWAJ) is a modified WSR-93 S-band (2780 MHz) scanning radar with a beam width of 1.12° and Doppler and dual-polarization capability upgrades. It is described in detail in Schumacher and Houze (2000) and Wolff et al. (2005).

3. VN software description

The VN software suite consists of three major components: 1) data ingest and preprocessing; 2) resampling of PR and GR to common 3-dimensional data volumes (creation of match-up data products); and 3) statistical analysis and display of the matching data volumes.

The data ingest and preprocessing component of the VN software ingests and stores TRMM PR and coincident ground radar data whenever an "overpass event" occurs. Such an event takes place any time the TRMM PR ground track passes within 200 km of a VN ground radar (GR) site. For each overpass event, the GR volume scan beginning at or just prior to the satellite overpass time is acquired along with its corresponding PR data. GR data are acquired for the WSR-88D sites on a routine, operational basis by the VN, via the TRMM Ground Validation Office. Data for other ground radar sites are currently acquired by the VN on an ad-hoc basis from the data providers. Subsets of the full-orbit PR data provided by the PPS for single radars or adjacent groups of radars are acquired by the VN. All data acquired by the VN are stored permanently in the VN file system, unmodified and in their native format. All acquired data files are cataloged in the VN in a PostGRESQL relational database.

Selected fields of the PR products are analyzed upon receipt to temporary 75-by-75 point Cartesian grids of 4-km resolution, one centered on each ground radar site overpassed by the TRMM satellite in the given orbit. The VN software harvests metadata parameters for each site overpass event from the temporary grids. These parameters serve to characterize the precipitation and radar echo characteristics of the event. The metadata are stored in the VN relational database and are linked through the database to the associated PR orbit subset and GR data files. Metadata parameters stored include the average height of the bright band over the analysis area, and the number of grid points:

- total, in a horizontal grid slice
- covered by the PR data swath: total for grid, and total within a 100 km radius of the GR site
- indicating Rain Certain: total, and within 100 km
- indicating convective rain type: total, and within 100 km
- indicating stratiform rain type: total, and within 100 km
- indicating rain type "other": total, and within 100 km
- indicating No Rain: total, and within 100 km
- indicating bright band exists: total, and within 100 km.

The time and distance of the nearest approach of the TRMM orbit track to the ground radar site, and the start time of the GR volume scan, are also stored in the database. Queries to the database allow an analyst to easily identify events with significant areal precipitation, precipitation of a given type (convective or stratiform, or unknown), or precipitation events where the orbital track is within a threshold distance of the ground radar. All associated PR and GR data files are cataloged in the database and linked to the site overpass events, making it easy to assemble the data files for significant events for detailed analysis, for download by investigators, etc. Most site overpass events will have no occurrence of precipitation echoes. The preprocessed metadata in the database makes it easy to select rainy overpass events without the need to process all the data or make complicated time/space associations to external data sources.

On average, about 48 coincident events with available matching PR and GR data are collected each month for each of the WSR-88D ground radars listed in Table 1. Due to their proximity to the top of the TRMM orbit, the northernmost sites in the table experience about twice the number of coincident overpasses as the southernmost sites.

Although PR and GR data products from every overpass event are acquired and stored, PR-to-GR match-up products are generated only when an overpass event occurs during a "significant precipitation event," as indicated in the stored metadata for the event. A significant precipitation event is defined as one in which at least 100 grid points within 100 km of the radar indicate Rain Certain (as defined in the PR product 2A-25). In the period from 8 August 2006 through 8 August 2008, a total of 25,032 coincident overpass events were recorded by the VN. Of these, 1,990 individual overpass events also met the rain area criteria. Thus, about 4 coincidence events per month per site meet the criteria for a VN rainfall event. Of these coincident events, about 3.5 per month per site have matching GR data available.

For those site overpass events meeting the significant precipitation event criteria, the resampling component of the VN software suite performs a geometric match-up of the PR and GR data. In this method, common 3-D volumes are defined by the intersection of the individual PR rays with the each of the conical elevation sweeps of the ground radar for the coincident GR volume scan. Thus, the resampled volume elements of the VN PR and ground radars can be directly compared to one another. This method is described in detail in Section 4. An earlier "legacy" version of the VN software used a comparison method based on resampling the data to a fixed 3-D Cartesian grid centered on the radar site. The legacy approach followed the analysis procedures described in Liao et al. (2001), with operational enhancements for the VN. Both the legacy and the current match-up software store the resulting PR-to-GR "match-ups" as netCDF files in the VN file system. The remainder of this paper is restricted to descriptions and results pertaining to the current geometric match-up version of the VN algorithm.

A statistical analysis and display component of the VN software suite generates statistical comparisons and graphical displays of PR and GR reflectivity factor and rain rate from the volume-matched data for a wide variety of data classifications. In many of the analysis and display programs, the data and results may be classified by individual attributes or combinations of attributes stored as, or derived from, variables stored within the netCDF files or the VN database. Attributes may apply to the entire data file, to a subset of the data in the file, or to an individual match-up sample volume. The primary attributes on which the data are classified typically include:

- GR site
- Date/Time ranges
- Height above the surface
- Proximity to the bright band (above, below, within)
- Precipitation type (Stratiform, Convective, Other)
- Underlying surface (Land, Water, Coast/Mixed)
- Range from the ground radar
- Percent completeness of the data volumes (expected vs. rejected gates, based on detection thresholds)
- Time difference between the PR and GR observations

4. VN netCDF product generation

The current algorithm to match PR and ground radar (GR) reflectivity data is based on calculating PR and GR averages at the geometric intersection of the PR rays with the individual GR radar elevation sweeps. By convention, the intersection points processed in the match-up are restricted to those where the intersection of the PR ray with the earth surface is within a 100 km radius of the GR site (Figure 1). Beyond 100 km, radar systems such as WSR-88D (1° beam width) will have a vertical resolution >1 km, which is considered too coarse for meaningful comparisons with the PR data.

The along-ray PR data are averaged only in the vertical, between the top and bottom height of each GR elevation sweep it intersects (Figure 2). The GR data are averaged only in the horizontal within the individual elevation sweep surfaces, over an approximately circular area centered on each intersecting PR ray's parallax-adjusted profile (Figure 3). Reflectivity is converted from dBZ to Z before averaging, then the average Z is converted back to dBZ. This technique thus averages the minimum number of PR and GR full-resolution space and ground radar bins needed to produce spatially-coincident sample volumes. The output of this technique is a set of vertical profiles for a given rainfall event, with coincident PR and GR samples located at essentially random heights along each individual profile. The vertical locations of the samples are not fixed because the technique selects the minimum volume for each coincident sample; there is no resampling to a regular grid. The advantages of the current technique over gridded approaches are that there is no interpolation, extrapolation, or oversampling of data, so matching volumes only exist at locations where both the PR and GR instruments have taken actual observations. Other than for the averaging required to produce the matching volumes, the data are not smoothed; and each sample volume carries a set of attributes that describe the precise spatial, temporal, and quality characteristics of the sample.

The VN software assigns the start time of each elevation sweep of the volume scan as the observation time for each sample of ground radar data within the sweep. For PR data, the time associated with each sample is the time of the PR's nearest approach to the ground radar, and is provided in a site coincidence table produced by the PPS. The orbital period of the TRMM spacecraft is 92.5 minutes, which yields a ground speed of about 7.22 km/sec. At that rate, the spacecraft ground track traverses a nominal ground radar radius of 200 km in only 28 seconds. This period is akin to a "snapshot" in comparison to either the time period required for the ground radar to complete its full volume scan, or the random time offset between the GR volume scan begin time and the PR overpass. The time difference between PR and GR samples is one of the potential sources of error in the match-up of meteorological events observed by these two datasets.

In summary, the PR data resolution is reduced in the vertical to the resolution of the GR, which varies with range from the ground radar, and varies in vertical coverage by the number of elevation sweeps of the ground radar. The GR data resolution is simply reduced and remapped in the horizontal to the PR's horizontal resolution and (ray,scan) coordinate system.

The input GR product consists of quality-controlled reflectivity data in either Universal Format (UF) data files (Barnes, 1980), a TRMM GV 1C-51 HDF file, or a legacy-format WSR-88D Level-II Archive data file (i.e., pre-super-resolution), each of which contains data for a single, complete volume scan.

VN output products are in the form of binary netCDF files containing the volume-matched PR and GR data. Each VN netCDF data file corresponds to a single site overpass event, and contains all the match-up data for the significant rain event. The basic structure of the VN netCDF match-up files is the same for all events. However, the dimensions of the data contained in the files vary, depending on the number of PR footprints that fall within a 100 km radius of the overpassed GR site for a given overpass event, and the number of unique elevation sweeps contained in the GR volume scan. In addition, the vertical and horizontal locations of the data points are unique for each event, and for each point within the event.

Horizontal and vertical positions of each data point in the geometry matching data set vary for each site overpass event as a function of the TRMM orbital track's variability and the ground radar's scan strategy (volume coverage pattern). Thus, each geometrically coincident PR and GR reflectivity data point in a given event has a unique set of associated horizontal and vertical position variable values. All latitude and longitude values are parallax-corrected for PR viewing angle and sample height. Multi-level variables in the data set (e.g., rain rate; number of 2A-25 points expected or rejected, see below) also have associated variables specifying the x- and y-corners of the PR footprint (in km, defined relative to a Cartesian coordinate system centered at the location of the ground radar, with the +y axis pointing due north), and the top and bottom height of the ground radar elevation sweep at the PR ray intersection point, in km above the surface. The PR footprint "corners" are defined as the midpoint between the footprint center point and the centers of the four diagonally-adjacent PR footprints, and are used only for graphical plotting of the match-up data, such as on Plan Position Indicator (PPI) image displays (e.g., Fig. 6).

One set of output match-up variables is concerned with the reflectivity and rain rate characteristics of the geometrically-coincident, full-resolution PR and GR radar range gates included in their respective volume averages. These "expected/rejected" variables provide a metric that can be used to assess the "goodness" of the match-up between the radars. For a given PR ray and GR sweep, several ground radar (GR) range gates and rays will typically intersect several PR range gates, as illustrated in vertical cross section in Figure 3. The geometry matching algorithm computes separate PR and GR volume-average values for all such intersecting PR and GR range gates, with the limitation that only those gates at or above specified reflectivity or rain rate thresholds are included in the PR and GR gate averages. This reflectivity threshold, while selectable, is typically set at 18 dBZ for PR (the minimum sensitivity level of the TRMM PR) and 15 dBZ for ground radars. Individual PR or GR samples falling below this threshold are "rejected," i.e., not included in the match-up volume averages. When generating volume average reflectivity and rain rate values for each match-up volume, the VN algorithm calculates: (a) the number of PR and GR gates *expected* to be included in the averages from a strictly geometric standpoint, and (b) the number of these PR and GR gates falling below the applicable measurement threshold and *rejected* from inclusion in the averages. These metrics are stored in variables in the match-up netCDF file. In statistical analyses of the data, effects of non-uniform beam filling and biases related to the detection threshold of the PR may be minimized by limiting the data points to those where the number of rejected gates is zero for both the GR and PR volume averages. See Figure 6 for an example of the effect of limiting the match-up data based on the percent of rejected points in the sample averages.

The *GPM Validation Network Data Product User's Guide* (NASA, 2009) provides detailed descriptions of the VN netCDF match-up data file format and content, including a more detailed description of the gates expected/rejected variables. Copies of the user's guide are available on-line from the GPM Ground Validation website: http://gpm.gsfc.nasa.gov/groundvalidation.html.

5. VN Software and Operations Requriements

The VN software system exists as a set of Linux shell scripts, PostgreSQL database utilities, SQL commands, and a body of code written in Interactive Data Language (IDL; www.ittvis.com). PR subset product and coincidence table data acquisition from the PPS, and cataloging, preprocessing, metadata extraction and storage for these products are automated within the VN software. GR data receipt and cataloging are automated for the WSR-88D sites, internal to the VN system, while WSR-88D data acquisition, quality control, and transmission to the VN system is a mix of automated and manual procedures, and is externally handled for the VN by the TRMM Ground Validation Office at NASA/GSFC. Due primarily to security constraints, GR data acquisition and processing for other GR sites are currently performed manually on an ad-hoc basis as data are made available by the provider, and use supporting scripts written for this purpose. Generation of the VN PR-GR match-up products is also performed on an ad-hoc basis, though it may be readily automated to meet timeliness requirements for the data in the GPM era.

The driving system requirements for the ability to run the VN software are a licensed copy of ID with a Linux or UNIX operating system or underpinnings (e.g., UNIX and X11 under Mac OS X). The PostgreSQL relational database management system (RDBMS) is required only for the operational data ingest, cataloging, and preprocessing component of the VN software suite, and is optional for the match-up product generation and statistical analysis and graphical display components. A different RDBMS could be substituted for PostgreSQL with minor software modifications. The Windows operating system is not supported by the baseline VN software. All VN processing and visualization software are designated "open source," and are available from the NASA/GSFC Innovative Partnerships Program Office website: http://opensource.gsfc.nasa.gov.

The VN data processing system and database are designed with the flexibility to add additional data products, ground radar sites, and metadata parameters. Any ground radar sites within the TRMM PR area of coverage may be supported within the current system as long as the reflectivity data are available in Universal Format or the WSR-88D Archive Level II format.

6. Analysis of VN Data

One of the key applications for VN data is in the validation of space-based measurements. VN data were therefore selected to compute the bias between the TRMM

Precipitation Radar (PR) and the NOAA WSR-88D Ground Radars (see Table 1 for a list of ground radars). In this analysis 2363 overpass events with significant rainfall were evaluated. The data were collected during the period from August 8, 2006 through March 22, 2009. All results to follow use the attenuation-corrected PR reflectivity from the TRMM 2A-25 product. In performing the analysis described below, the data were first stratified into convective and stratiform cases, based on the Rain Type flag derived from the TRMM 2A-23 product. For stratiform cases, the data were further restricted to samples where:

- The bright band exists for a given PR profile (as defined by the BBheight parameter, derived from the PR 2A-25 product)
- The PR reflectivity factor exceeded 18 dBZ, which is the instrument's minimum usable sensitivity
- The match-up of GR and PR samples have no "rejected" bins in their volume averages (see description of expected/rejected observations in Section 4)
- The fraction of rain-producing PR profiles within a given rain event was >80% stratiform.

A similar set of criteria were applied to the convective cases, with the exception that the bright band rule was not applied, and rain events were excluded if the portion of rain-producing PR profiles in the event was less than 30% convective. The data were further stratified into separate classes of samples from above and below the melting layer (bright band). Samples with bottom heights greater than 0.5 km and top heights 2 km or more below the average bright band height were assigned to the "below bright band" class. Samples with bottom heights 2 km or more above the average bright band height were assigned to the "above bright band" class. Each included point is given equal weight in the bias computations.

In all cases, the radar frequency corrections defined by Liao and Meneghini (2009) were applied to the GR data to account for the differences in reflectivity factor that occur when the same rain or snow targets are observed by S- and Ku-band radars. The snow correction was applied to data above the bright band, and the rain correction was applied to the data samples below the bright band. In all, 1,850,228 volume-matched samples were available. Given the restrictions described above, many fewer samples were actually included in the analysis. The sample sizes for each data subclass are identified in Table 2.

The stratiform points above the bright band are the echo areas where the best agreement is expected between the PR and the GR radar, where PR attenuation is minimal, and where convective reflectivity gradients and bright band effects are not a factor. In our study, the assumptions are that the PR is stable and well-calibrated, and the mean differences between the PR and GR for the stratiform/above bright band case are primarily due to GR calibration offsets. As illustrated in Figure 4, the PR average reflectivity is remarkably consistent with the corrected GR reflectivity factor, especially in the stratiform cases. In this figure, the average PR minus corrected GR radar reflectivity factor is plotted against the maximum PR reflectivity factor in the profile from which the sample was collected. There are two horizontal lines drawn in each plot in this figure, one illustrating zero bias and a second that illustrates the mean value of PR-GR (frequency corrected, in the above and below bright band cases) for the ensemble of samples plotted in each graph.

Table 2 summarizes the bias calculations for the convective and stratiform cases above and below the bright band. The magnitude of absolute difference in average PR and GR reflectivity is relatively small: less than ±1.5 dBZ in each individual case, and equal to -0.2 dBZ when averaged over all cases.

Table 3 presents the PR-GR bias for individual ground radars, for both the frequency-corrected GR reflectivity and the original S-band GR reflectivity. This dataset is slightly less restrictive than in Table 2, and contains all samples categorized as stratiform rain type, with bottoms 500 m or more above the bright band, and where the percentage of PR and GR bins rejected as "below threshold" in the sample averages is below five percent. Events where fewer than 5 points meet the criteria are excluded from the results..

The frequency-corrected biases for most radar sites in Table 3 are less than 1 dBZ, with a few notable exceptions. KGRK (Fort Hood, Texas) shows a positive PR-GR bias over the full data set, indicating a negative calibration offset in the KGRK radar relative to other WSR-88D sites. Several adjacent WSR-88D sites near or along the Gulf coast between Louisiana and Florida (KLCH, KLIX, KSHV, KTBW, KTLH) exhibit a PR-GR bias of -1 dBZ or lower, indicating a high calibration offset of the WSR-88D radar. This set of Gulf coast radars, KEVX and KMOB excepted, seem to be well calibrated to one another, but run "hot" compared to the other WSR-88D sites in the VN subset. It is unknown to what extent these results represent actual calibration offsets, and to what degree the Gulf coast meteorological regime contributes to the observed offsets.

Another potentially useful application of the VN data is to track the absolute calibration of ground radars over time. Figure 5 shows a time series of mean PR-GR reflectivity differences for each WSR-88D site in the VN, and for the University of Alabama, Huntsville, ARMOR dual-polarimetric C-band radar (labeled RMOR) from July 2006 through March 2009. Figure 5 uses the same criteria as in Table 3 (stratiform rain, above bright band, having five percent or fewer bins below threshold in sample averages), with the additional constraint that, to reduce noise, at least 25 sample points must meet the criteria for the event to be included in the plot. A simple average of the event-by-event biases plotted in Fig. 5 cannot be directly compared to the accumulated mean biases in Table 3, as Table 3 takes the number of samples in each event into account in the mean difference computations, and the number of qualifying samples per event can vary by over an order of magnitude.

While KGRK shows a negative GR bias with respect to the PR over the full dataset as seen in Table 3, Figure 5 shows that the events with the consistently negative biases occur prior to mid-2007, and KGRK had improved to near-zero mean bias after mid-2007. KGRK and RMOR are the only sites that show a clear trend in the GR calibration. It is known that the calibration of the ARMOR data provided to the VN was improved between the early events and the later dates (W. Petersen, personal communication).

Several sites (KAMX, KBYX, KCRP, KMLB) show consistent, small biases with respect to the PR, indicating a stable calibration of the WSR-88D. These sites also generally have fewer rainy events meeting the criteria for inclusion, which may help reduce the variability. It is our intent to obtain the calibration adjustment records for the WSR-88D sites in the VN to compare to the observed reflectivity biases.

Visualization Tools for Case Studies

A suite of visualization tools has been developed for viewing and analyzing the VN geometry match-up data sets for individual site overpass events. The two primary tools are the statistical analysis tool and the vertical cross section tool. Noting that the match-up data are organized in the vertical by the elevation sweeps of the ground radar, with the horizontal sampling defined by the (ray,scan) coordinates of the TRMM PR, the data lend themselves to rendering as traditional Plan Position Indicator (PPI) images. As with traditional PPI images from a scanning ground radar, the height above ground and the vertical depth of the match-up samples plotted in the PPI display increase with distance from the ground radar.

An example of the PPIs of PR and GR reflectivity rendered from the geometry match data for a rainy TRMM PR overpass event at KAMX (Miami, Florida WSR-88D) for TRMM orbit 61300 on 18 August 2007 around 22:18 UTC is shown in Fig. 6. The figure shows PR and GR PPIs corresponding to the 1.8° elevation sweep of the ground radar, where the plotted match-up samples have been restricted to those where, for both the PR and GR, fewer than 5% of the gates averaged to produce the sample were rejected as being below fixed thresholds (18 dBZ for PR, 15 dBZ for GR) defined in the match-up algorithm. In this case of widespread, predominantly stratiform precipitation the effect of the threshold restriction is minimal. Figure 6 is an example of the interactive PPI image display as output by the vertical cross section tool. As in the preceding section, all example displays and statistics below are based on attenuation-corrected PR data from the TRMM 2A-25 product.

The statistical analysis tool also displays user-selected PPIs as shown in Fig. 6, in the form of an animation loop progressing from low to high elevation sweeps. The statistical analysis tool stratifies the event data into vertical layers in two manners: (1) by height above the surface, in 1.5-km-deep layers, for 15 levels centered from 1.5 to 19.5 km, and (2) into three layers defined by proximity to the bright band (freezing level): above, within, and below the bright band. For purposes of the latter, match-up samples are categorized as above (below) the bright band if their base (top) is 500 m or more above (750 m or more below) the mean bright band height. The remaining points are assigned as within the bright band. The mean bright band height is computed from the bright band analysis in the TRMM PR 2A-25 product. When the area of stratiform rainfall is not deep and widespread, this analysis can be an overestimate of the observed bright band height in the PR reflectivity, in particular for the southernmost radars in the southeastern U.S. Thus, for purposes of the statistical analysis of the match-up data the bright band area of influence is extended further below the mean bright band height than above to reduce the possibility of including bright band affected data samples in the below-bright-band category.

The statistical analysis tool uses the vertically-stratified data to produce a number of tabular and graphical displays. The upper left panel in Fig. 7 shows vertical profiles of PR (thick lines) and GR (narrow lines) reflectivity from match-up data averaged over the constant height levels. The remaining 3 panels in Fig. 7 display histograms of PR and GR reflectivity accumulated in 2 dBZ bins for match-up data stratified by proximity to the bright band: below (upper right panel), within (lower left), and above (lower right). Table 4 presents PR-GR mean difference statistics output by the statistical analysis tool for data at the constant height levels broken out by rain type. The tool produces the same statistics broken out by proximity to the bright band. Separate profile and histogram plots are produced for sample points identified as stratiform (solid lines) and convective (dotted lines) rain type, as well as for all points without regard to rain type (not shown). Figure 8 shows the scatter plots of PR and GR reflectivity produced by the statistical analysis tool. Again the data are stratified by rain type and proximity to the bright band. The data samples included in Figs. 7 and 8 are limited to where at least 95% of the gates averaged to produce the match-up samples are above fixed thresholds for both the PR and GR sample.

Both the vertical profile and histograms show good agreement between the PR and GR reflectivities for stratiform rain samples above and below the bright band in the mean. PR-GR reflectivity bias, computed as the mean difference for matching points, was -0.85 dBZ for the stratiform, below bright band case, and -0.43 dBZ for the stratiform points above the bright band, with near-identical reflectivity distributions. The vertical profiles for this stratiform subset of samples exhibits a characteristic frequently seen in the case of a well-formed bright band, in that the GR profile is more affected by the presence of the bright band than the PR profile. Note the jump in GR reflectivity near the bright band level in the stratiform profile in Fig. 7 is much more pronounced than for the PR. The mean PR-GR reflectivity difference for stratiform rain increases to -1.76 dBZ for points within the bright band.

The scatter diagrams in Fig. 8 show that there can be significant differences between the PR and GR match-up samples on a point-by-point basis, though the data heavily cluster along the 1:1 line. These differences are due to a combination of factors, including differences in viewing geometry and radar frequencies, errors in vertical (for GR) and horizontal (for PR) geolocation of the data, and errors in the PR attenuation correction. The tools allow the S-to-Ku band frequency adjustment of Liao and Meneghini (2009) to be applied to the GR reflectivity data for points above (snow correction) and below (rain correction) the bright band. These corrections result in degradation of the PR-GR reflectivity bias to -2.02 dBZ for the stratiform, below bright band case, but improve the bias to -0.08 dBZ for the stratiform points above the bright band, indicating that the attenuation correction for the PR is underperforming for this case.

The vertical cross-section tool generates cross sections of the PR and GR reflectivity match-up data and PR-GR reflectivity difference along a selected PR scan line (perpendicular to the TRMM orbit track). Figure 9 shows vertical cross sections of PR reflectivity and PR-GR reflectivity difference for match-up data taken along the PR scan line indicated by the A-B line shown in Fig. 6, under the same data constraints as Figs. 6-8, but with the S-to-Ku band frequency adjustment applied to the GR reflectivity. The cross section passes through a convective core with match-up sample reflectivities up to 49 dBZ for the PR and 54 dBZ for the GR. The difference cross section shows that the per-sample PR reflectivity is generally within 1-2 dBZ of the GR above the bright band level, with the GR reflectivity exceeding the PR within and below the bright band, especially within the convective core.

The vertical cross section tool in IDL is interactive, and its primary user interface is the PR/GR PPI image pair display as shown in Fig. 6. Clicking the mouse on a point within the PPI image launches a new set of PR, GR, and PR-GR reflectivity cross sections along the PR scan line through the selected point. If the original 2A-25 TRMM PR product files are available, cross sections of full-vertical-resolution (250 m) PR data can also be displayed for comparison to the vertically-averaged PR match-up data. Clicking on the labeled white boxes in the upper right corner of the GR PPI allows the user to toggle the S-to-Ku band adjustment on and off, and increment and decrement the GR reflectivity in 1 dBZ steps to eliminate a known GR calibration offset from the cross section displays. To investigate the quality of the PR and GR geometric alignment, the user can also click in the lower left white box to launch a PPI animation sequence of PR and GR match-up data, and if the data files are available, full-resolution GR PPIs created from the original GR data volume.

7. Summary and conclusions

As described above, the Validation Network is an integral part of the Ground Validation System for NASA's Global Precipitation Mission (GPM). In the GPM pre-launch era, the VN supports precipitation retrieval algorithm development. Post-launch, the VN will be used to validate GPM spacecraft instrument measurements and retrieved precipitation data products.

Several examples are provided above that demonstrate how the VN dataset can be used to compare ground to space-based radar reflectivity for validation purposes. Examples include comparisons in individual storms, in a time series of storms over individual ground radars, and in a multi-year aggregate of storms over the entire southeast U.S.

Analysis of individual storms illustrates several of the key features of the VN. Chief among these is the "match-up" method that permits direct comparison of volume-averaged ground- and space-based radar data. The VN algorithm averages the minimum number of full-resolution space and ground radar bins needed to produce spatially-coincident sample volumes. Space-based radar data are averaged only along each vertical ray, between the top and bottom height of each ground radar elevation sweep that it intersects (Figure 2). Ground radar data are averaged only in the horizontal within the individual elevation sweeps that intersect the space radar rays' parallax-adjusted profiles (Figure 3). The result of this technique is a set of vertical profiles for a given rainfall event, at the PR horizontal resolution and location and the GR vertical resolution and location, with coincident space and ground radar samples located at essentially random heights along each individual profile (Figure 9). There is no data interpolation, extrapolation, or resampling to a regular grid.

The analysis of individual storms also illustrates the standard VN products generated for each rain event. These include PPI images, vertical profiles, histograms, scatter diagrams, and mean difference statistics for PR and GR reflectivity, as shown in Figs. 6-8 and Table 4. It should be noted that data points included in the standard match-up that generated these figures (and the other analysis described here) are limited to those that fall within a 100 km radius centered on the ground radar. Beyond 100 km, radar systems with a 1° beam width (such as WSR-88D) will have a vertical resolution >1 km, which is considered too coarse for meaningful comparisons with the space-based radar data such as those available from TRMM and GPM.

Examples provided above also illustrate the utility of the VN dataset as a means for assessing the long-term calibration of ground radars. The period of record for the VN prototype begins on August 8, 2006 and runs to the present for the 21 ground radar sites located in the southeast U.S. (Figure 1). Table 3 and Figure 5 show that for this period of record the frequency-corrected bias between the TRMM Precipitation Radar (PR) and WSR-88D ground radars (GR) is less than 1 dBZ in most cases, with several notable exceptions. For example, it was found that several adjacent WSR-88D sites near or along the Gulf coast between Louisiana and Florida exhibit a Precipitation Radar (PR) minus Ground Radar (GR) reflectivity factor bias of -1 dBZ or lower, indicating a high calibration offset for these WSR-88D ground radars. This set of Gulf coast radars (KEVX and KMOB excepted) appears to be well calibrated to one another, but run "hot" compared to the other WSR-88D sites in the VN subset. It is beyond the scope of this investigation to determine whether these results represent actual calibration offsets, or to what degree the Gulf coast meteorological regime contributes to the observed offsets.

An assessment was also made of the overall PR-to-GR bias for all 21 southeast U.S. ground stations, drawing on the more than $1.8\mathrm{x}10^6$ individual PR-to-GR match-up samples in this period of record. As illustrated in Figure 4 and Table 2, the PR average reflectivity is remarkably consistent with the frequency-corrected GR reflectivity factor, especially in the stratiform cases. The magnitude of absolute difference in average PR minus GR reflectivity is relatively small for stratiform rain: equal to -0.2 dBZ when averaged over all above- and below-bright-band cases.

Several steps have been taken to make the VN dataset as accessible as possible for GPM algorithm development and for data product validation. Summary data products are available for each precipitation event. Ground radar data can be ingested into the VN if it is in the relatively commonly used Universal Format (UF) or in WSR-88D data format. The VN data itself are formatted as netCDF, a portable, self-describing data format that is commonly used in the atmospheric sciences. A data user's guide is available that details the VN data file naming conventions, format, and contents (http://gpm.gsfc.nasa.gov/ground_library.html). Space- and ground-radar match-up data are available for each significant rain event, and raw data for each overpass event are available by request from the authors. A VN data visualization tool is available that renders the match-up data in vertical "plan position indicator" slices through the data, where each slice can be located in an arbitrary horizontal orientation. The VN visualization tool, written in Interactive Data Language (IDL), is available as open source software from the NASA/GSFC Innovative Partnerships Program Office website: http://opensource.gsfc.nasa.gov. Indeed, the entire suite of VN software is available as open source from the same url location..

Additional data will certainly be added to the VN as the period of record expands. Enhancements to the VN are also planned, with the possibility of expanding the period of record to dates earlier than August 8, 2006, and with the possibility of adding additional data types, including space-based microwave radiometer data, as well as additional data derived from various precipitation retrieval methods. Community contributions that improve and enhance the open source VN software are welcome, as are contributions of ground radar data from additional sites. Updates to the VN will be documented on the GPM ground validation website (http://gpm.gsfc.nasa.gov/groundvalidation.html). This site provides a portal to VN contacts, data, software, and documentation, as well as to other ground validation datasets, both within and beyond GPM.

8. Acknowledgement

The Validation Network is supported as part of NASA's Global Precipitation Measuring Mission.

9. References

Anagnostou, E.N., C.A. Morales, and T. Dinku, 2000: The use of TRMM Precipitation Radar observations in determining ground radar calibration biases. *J. Atmos. Ocean. Tech.*, **18**, 616-628.

Barnes, S. L. (1980): Report on a meeting to establish a common Doppler radar data exchange format. *The Bulletin of the American Meteorological Society*, Vol. 61, No. 11, 1401-1404

Bolen, S.M. and V. Chandrasekar, 2000: Quantitative cross validation of space-based and ground-based radar observations. *J. Appl. Meteor.,* **39**, 2071-2079.

Bolen, S.M. and V. Chandrasekar. 2003. Methodology for aligning and comparing spaceborne radar and ground-based radar observations. Journal of Atmospheric and Oceanic Technology 20:647-659.

Conover, W.J. 1980, *Practical Nonparametric Statics*. 2nd edition. John Wiley and Sons, Inc.

GEO, 2005. Global Earth Observation System of Systems GEOSS. Group on Earth Observations. GEO 1000R/ESA SP-1284. February 2005. ISBN 92-9092-986-3.

GCOS, 2006, *Systematic Observation Requirements for Satellite-based Products for Climate—Supplemental details to the satellite-based component of the Implementation Plan for the Global Observing System for Climate in Support of the UNFCCC (GCOS-107)*, September 2006.

Hou, A.Y., Gail Skofronick-Jackson, Christian D. Kummerow, James Marshall Shepherd, 2008, Global precipitation measurement, Chapter 6 in *Precipitation: Advances in Measurement, Estimation and Prediction*, S.C.Michaelides, ed., Springer-Verlag, 540 p. 38 illus., 23 in color., Hardcover, ISBN: 978-3-540-77654-3

Keenan, T., K. Glasson, F. Cummings, T.S. Bird, J. Keeler and J. Lutz, 1998: The BMRC/NCAR C-Band Polarimetric (C-POL) Radar System. J. Atmos. and Oceanic Tech., **15**, 871-886.

Kozu, T., Toneo Kawanishi, Hiroshi Kuroiwa, Masahiro Kojima, Koki Oikawa, Hiroshi Kumagai, Ken'ichi Okamoto, Minoru Okumura, Hirotaka Nakatsuka, and Katsuhiko Nishikawa. IEEE TRANSACTIONS ON GEOSCIENCE AND REMOTE SENSING, VOL. 39, NO. 1, JANUARY 2001. Development of Precipitation Radar Onboard the Tropical Rainfall Measuring Mission (TRMM) Satellite.

Liao, L., R. Meneghini, 2009: Changes in the TRMM Version-5 and Version-6 Precipitation Radar Products due to Orbit Boost. Journal of Meteorological Society of Japan. Complete citation to be added.

Liao, L., R. Meneghini, and T. Iguichi, 2001: Comparisons of rain rate and reflectivity factor derived from the TRMM Precipitation Radar and the WSR-88D over the Melbourne, Florida, site. *J. Atmos. Ocean. Tech.*, **18**, 1959-1974.

NAS, 2007. Earth Science and Applications from Space: National Imperatives for the Next Decade and Beyond. National Academy Press. ISBN: 0-309-66714-3.

NASA, 2009. Validation Network Data User's Handbook.

Neek and Oki, 2007.

NOAA, 2006. U.S. Dept. Commerce, NOAA, OFCM, 2006. Federal Meteorological Handbook No. 11 (FMH-11) - Doppler Radar Meteorological Observations (WSR-88D), Part C - WSR-88D Products and Algorithms (390 pp.). Office of the Federal Coordinator for Meteorological Services and Supporting Research (OFCM), National Oceanic and Atmospheric Administration. Online at http://www.ofcm.gov.

Park, S.-G., and D.-K. Lee. 2007. Doppler weather radar network over the Korean peninsula. P11A.5. 33rd Conference on Radar Meteorology. Cairns, Australia. 6-10 August.

Petersen, W. A., K. R. Knupp, D. J. Cecil, and J. R. Mecikalski, 2007: The University of Alabama Huntsville THOR Center instrumentation: Research and operational collaboration. 33rd International Conference on Radar Meteorology, American Meteorological Society, Cairns, Australia, August 6-10, 2007.

Rosenfeld, D., E. Amatai, and D.B. Wolff. 1995. Journal of Applied Meteorology. 34:198-211. Classification of Rain Regimes by the Three-Dimensional Properties of Reflectivity Fields.

Schumacher, C., and R. A. Houze, Jr., 2000: Comparison of radar data from TRMM satellite and Kwajalein oceanic validation site. J. Appl. Meteor., **39**, 2151-2164.

Simpson, J., C. Kummerow, W.-K. Tao, and R.F. Adler, 1996. On the Tropical Rainfall Measuring Mission (TRMM). Meteorology and Atmospheric Physics 60:19-36.

Smith, E.A., G. Asrar, Y. Furuhama, A. Ginati, C. Kummerow, V. Levizzani, A. Mignai, K. Nakamura, R. Adler, V. Casse, M. Cleave, M. Desbois, J. Durning, J. Entin, P. Houser, T. Iguchi, R. Kakar, J. Kaye, M. Kojima, D. Lettenmaier, M. Luther, A. Metha, P. Morel, T. Nakazawa, S. Neeck, K. Okamoto, R. Oki, G. Raju, M. Shepherd, E. Stocker, J. Testud, and E. Wood. 2006. International Global Precipitation Measurement (GPM) Program and Mission: An Overview. In *Measuring Precipitation from Space: EURAINSAT and the Future* (V. Levizzani and F.J. Turk, eds.). Kluwer Publishers, Dordrecht, The Netherlands.

Wolff, D. B., D. A. Marks, E. Amitai, D. S. Silberstein, B. L. Fisher, A. Tokay, J. Wang, and J. L. Pippitt, 2005: Ground validation for the Tropical Rainfall Measuring Mission. *J.*

Atmos. Ocean. Tech, 22, No. 4, 365-380.

Figure Captions

Figure 1. Location of Validation Network WSR-88D match-up sites in the southeastern U.S. 100 km observation limits are illustrated for each site.

Figure 2. Schematic of PR gate averaging at GR sweep intersections. Shaded areas are PR gates intersecting two GR sweeps (dashed) at different elevation angles. Only one PR ray is shown.

Figure 3.Illustration of the intersection of TRMM Precipitation Radar (PR) and WSR-88D Ground Radar (GR) sample volumes in the near range (left) and far range (right). The projection of these intersections along a PR ray is illustrated below, again for the near and far ranges (left and right sides, respectively).

Figure 4. Scatter plot of PR minus GR radar reflectivity factor for all samples measured over the NOAA WSR-88D radars illustrated in Figure 1, over the entire VN period of record. Convective and stratiform cases above, within and below the melting layer (bright band) are illustrated. The zero-bias line is plotted as well as the average PR-GR radar reflectivity factor for each case.

Figure 5. Time series of PR-GR mean reflectivity differences for stratiform rain above the bright band. Individual rain event dates are shown by the asterisks. The solid (dashed) line shows differences based on unadjusted (S-to-Ku frequency-adjusted) GR. Only GR-unadjusted difference values are plotted for RMOR, a C-band radar.

Figure 6. Geometrically-matched PR (top) and KAMX WSR-88D (bottom) data for the 1.8° elevation sweep of KAMX radar at 22:18 UTC on 18 August 2008, rendered as PPIs. Data samples shown are restricted to those points-in-common where at least 95% of the gates making up the sample averages were above fixed thresholds of 18 dBZ for PR and 15 dBZ for GR. Hatching shows PR-indicated rain type: vertical for convective, horizontal for stratiform. Rejected data points are shown by hatched pattern with dark gray color. Range rings are at 50 and 100 km. Edge of PR data swath is seen as the blank area to the south-southeast and inside 100 km. Line labeled A-B indicates the location of the vertical cross sections shown in Fig. 9.

Figure 7. Vertical profile (upper left panel) and histograms of geometrically-matched PR (heavy lines) and GR (narrow lines) reflectivity samples for the case shown in Figure 6. Stratiform (convective) rain type is plotted as solid (dotted) lines. Separate histograms are plotted for sample points below (upper right), within (lower left) and above (upper right) the bright band. Vertical scale varies in the histograms. PR-GR mean differences (bias, in dBZ) and sample sizes, by rain type, are indicated for the data in each histogram. Histogram bin width for accumulations is 2 dBZ. Points are limited to where at least 95% of the gates averaged to produce the PR and GR match-up samples are above fixed thresholds (see Fig. 6 and text). Dashed horizontal line in the vertical profile indicates the mean bright band height as analyzed in the TRMM PR 2A-25 product.

Figure 8. Scatter plots of PR vs. GR reflectivity for the case and data constraints shown in Figs. 6 and 7. Solid lines indicate the 1:1 match, dashed lines indicate +/- 3 dBZ bounds, and dotted lines are the linear fit to the data.

Figure 9. Vertical cross section, from 0-20 km height, of PR reflectivity (top) and PR-GR reflectivity difference (bottom) from geometrically-matched PR and GR data along the PR scan line labeled A-B in Fig. 6. GR data have had S-to-Ku band adjustments applied. PR data shown in gray show sample points rejected based on the threshold criteria of Fig. 6. Vertical extent of samples in the lower elevation sweeps has been adjusted to eliminate overlaps in the plots. The heavy dashed line indicates the mean bright band height, and dotted lines plotted 500 m above and 750 m below this height indicate the area of influence of the bright band (see text).

Table Captions

Table 1. Ground radar sites included in the current GPM GVS Validation Network.

Table 2. Mean, μ, and standard deviation, σ, of Precipitation Radar (PR) instrument bias compared to WSR-88D Ground Radar (GR) measurements for samples from above, within, and below the melting layer (bright band, BB). The bias was calculated as PR minus GR reflectivity factor for match-up samples. Bias estimates are based on the use of GR data corrected as described in the text; results using uncorrected GR data are in parentheses. The sample size, n, is identified for each case.

Table 3. Mean Precipitation Radar (PR) instrument bias compared to WSR-88D Ground Radar (GR) measurements for samples from above the melting layer, by GR site. The bias was calculated as PR minus GR reflectivity factor for match-up samples. Bias estimates are shown for both frequency-corrected GR data (GR_{Ku}) and uncorrected GR data. The sample size is identified for each site.

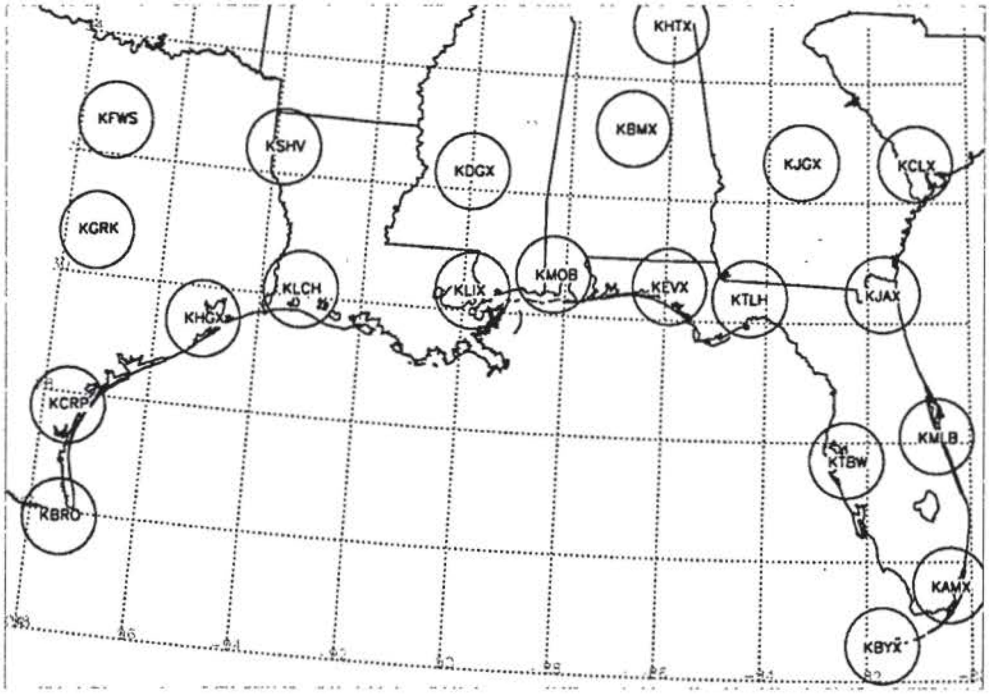

Figure 1. Location of Validation Network WSR-88D match-up sites in the southeastern U.S. 100 km observation limits are illustrated for each site.

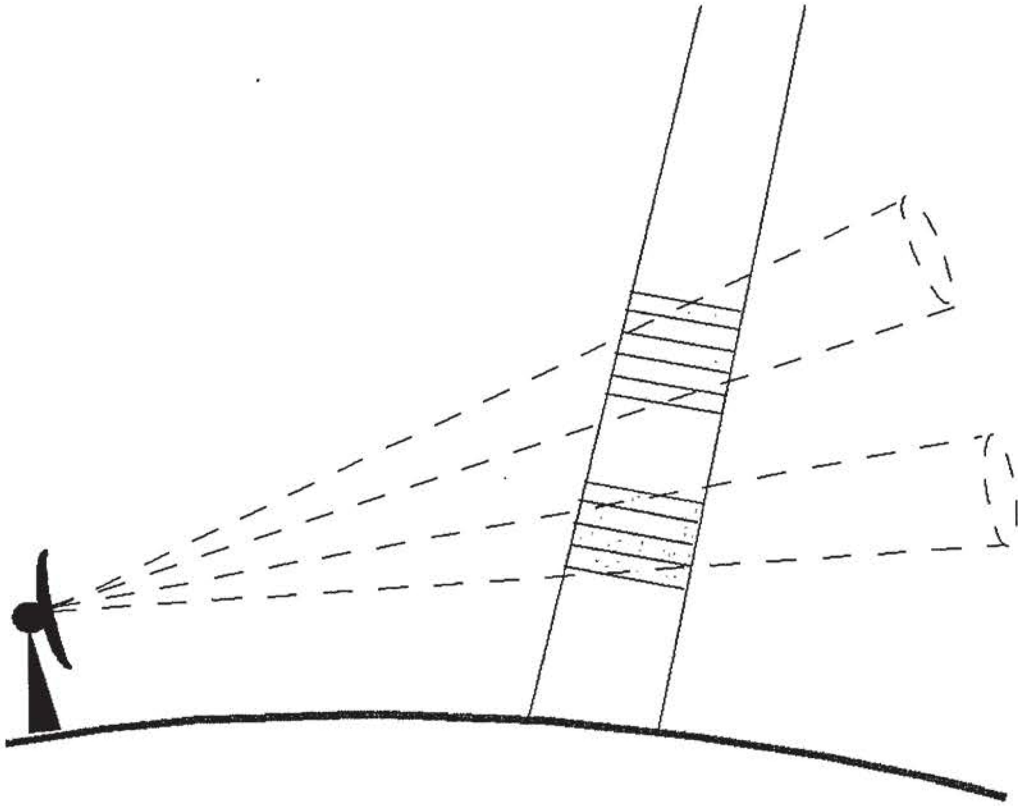

Figure 1. Schematic of PR gate averaging at GR sweep intersections. Shaded areas are PR gates intersecting two GR sweeps (dashed) at different elevation angles. Only one PR ray is shown.

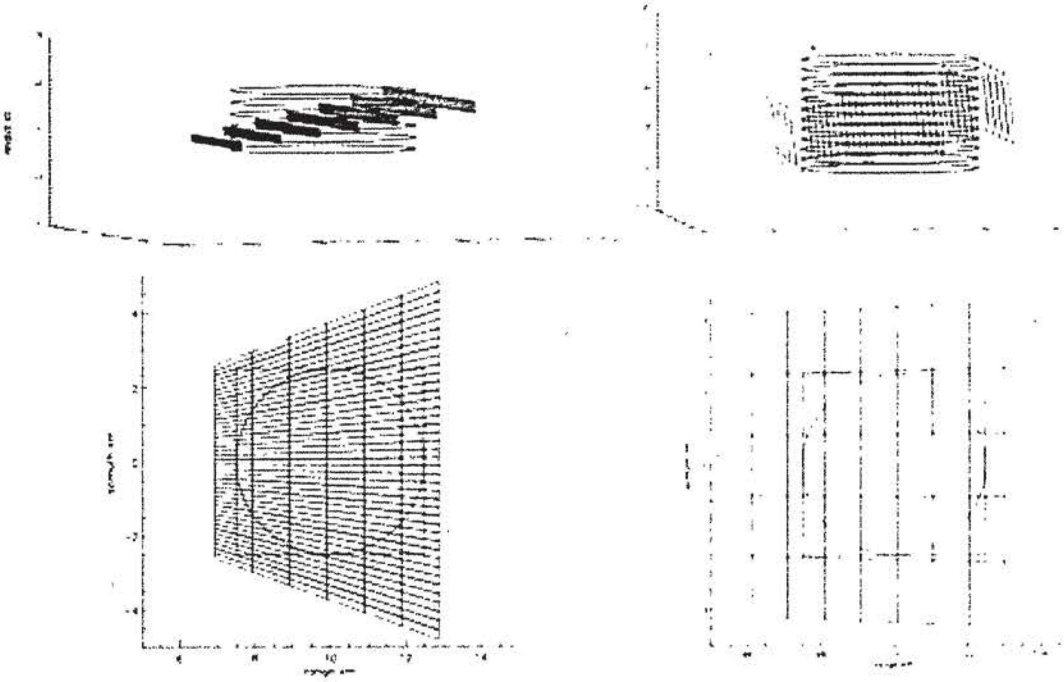

Figure 3. Illustration of the intersection of TRMM Precipitation Radar (PR) and WSR-88D Ground Radar (GR) sample volumes in the near range (left) and far range (right). The projection of these intersections along a PR ray is illustrated below, again for the near and far ranges (left and right sides, respectively).

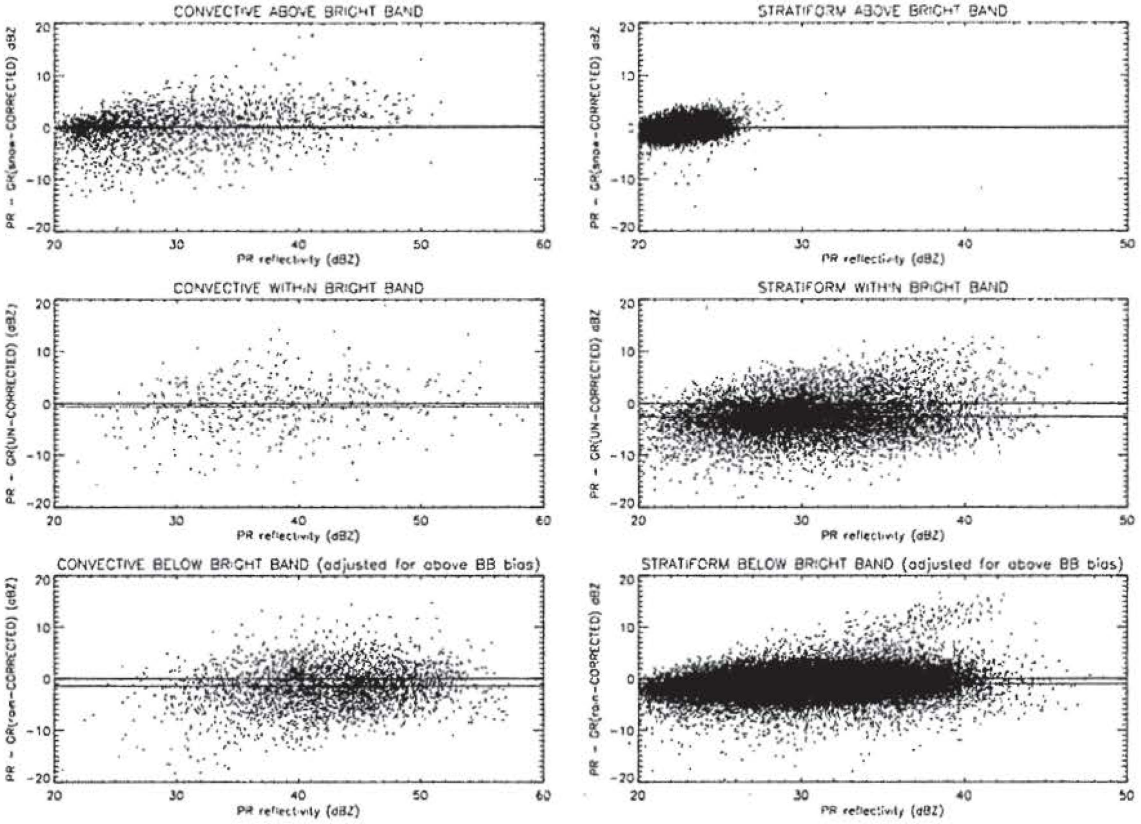

Figure 4. Scatter plot of PR minus GR radar reflectivity factor for all samples measured over the NOAA WSR-88D radars (see Figure 1), over the entire VN period of record. Convective and stratiform cases above, within and below the melting layer (bright band) are illustrated. The zero-bias line is plotted as well as the average PR-GR radar reflectivity factor for each case.

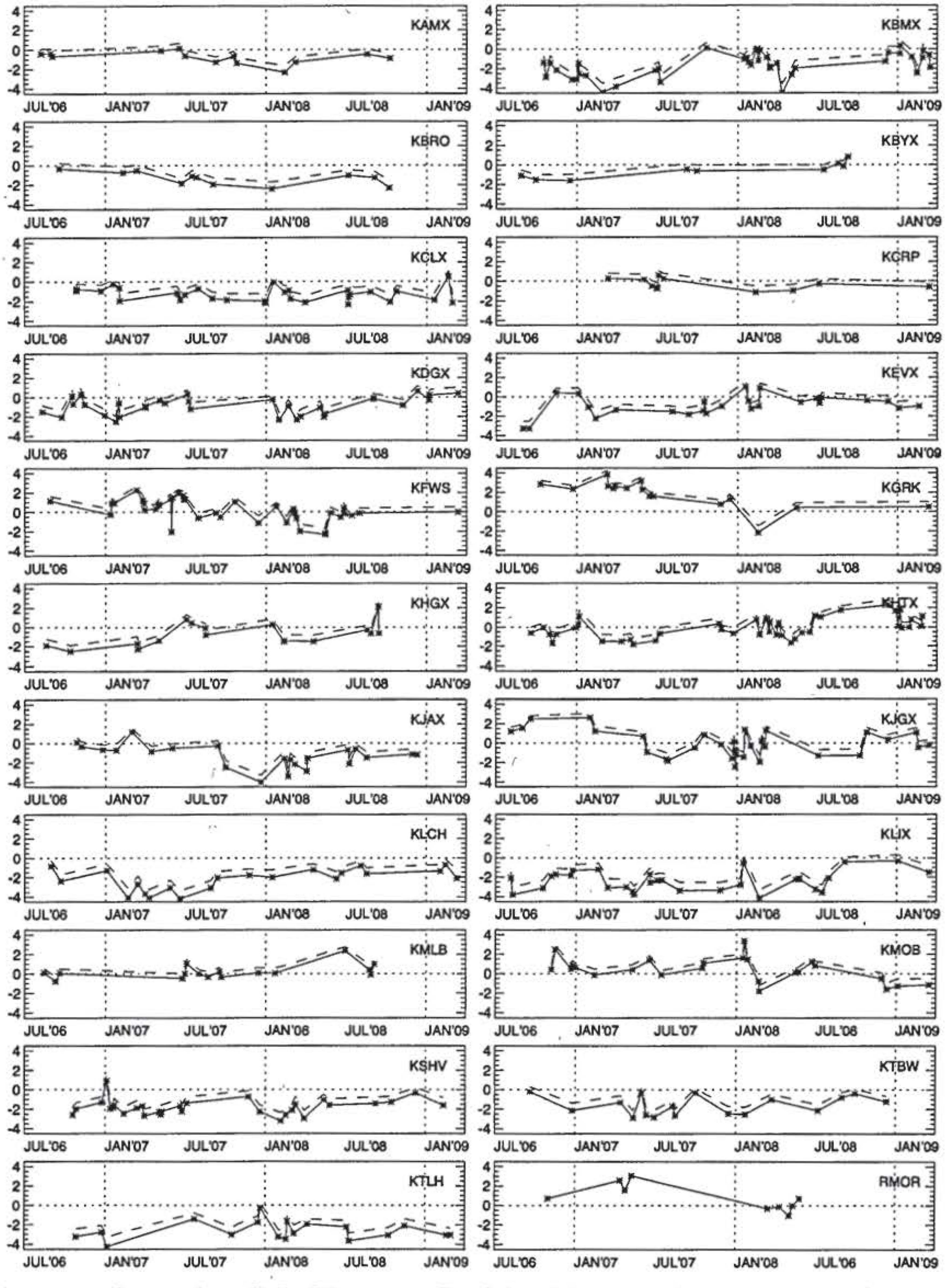

Figure 5. Time series of PR-GR mean reflectivity differences, in dBZ, for stratiform rain above the bright band. Individual rain event dates are shown by the asterisks. The solid (dashed) line shows differences based on unadjusted (S-to-Ku frequency-adjusted) GR. Only GR-unadjusted difference values are plotted for RMOR, a C-band radar.

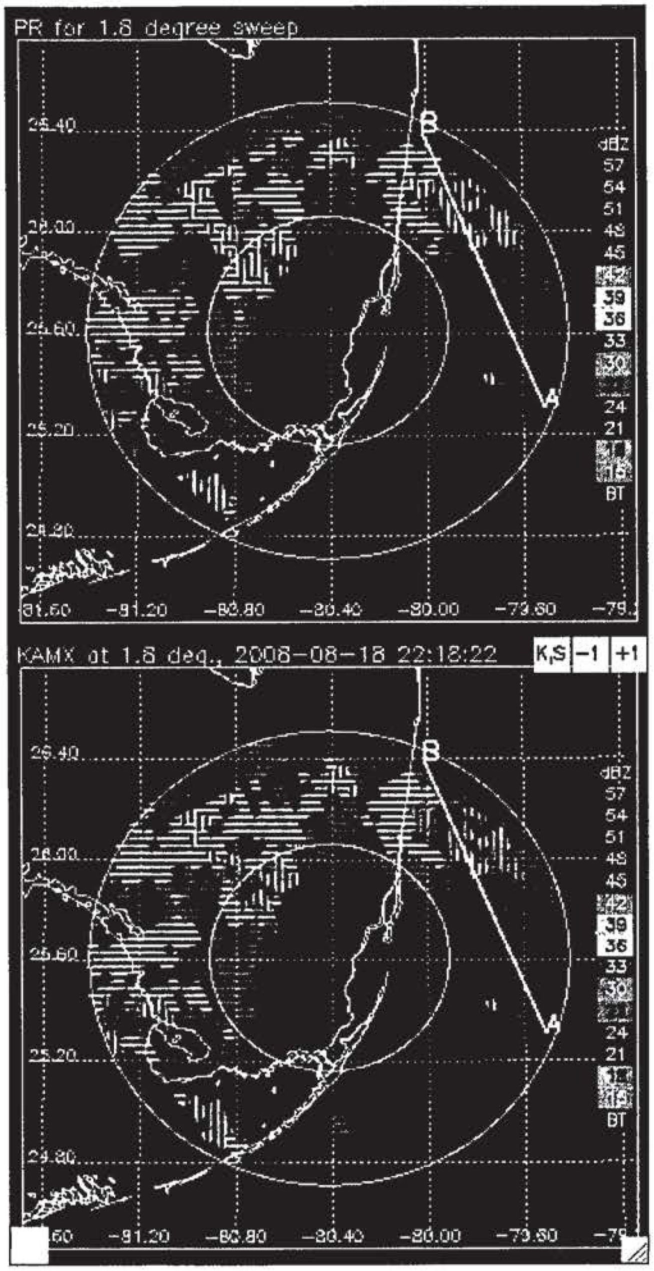

Figure 6. Geometrically-matched PR (top) and KAMX WSR-88D (bottom) data for the 1.8° elevation sweep of KAMX radar at 22:18 UTC on 18 August 2008, rendered as PPIs. Data samples shown are restricted to those points-in-common where at least 95% of the gates making up the sample averages were above fixed thresholds of 18 dBZ for PR and 15 dBZ for GR. Hatching shows PR-indicated rain type: vertical for convective, horizontal for stratiform. Rejected data points are shown by hatched pattern with dark gray color. Range rings are at 50 and 100 km. Edge of PR data swath is seen as the blank area to the south-southeast and inside 100 km. Line labeled A-B indicates the location of the vertical cross sections shown in Fig. 9.

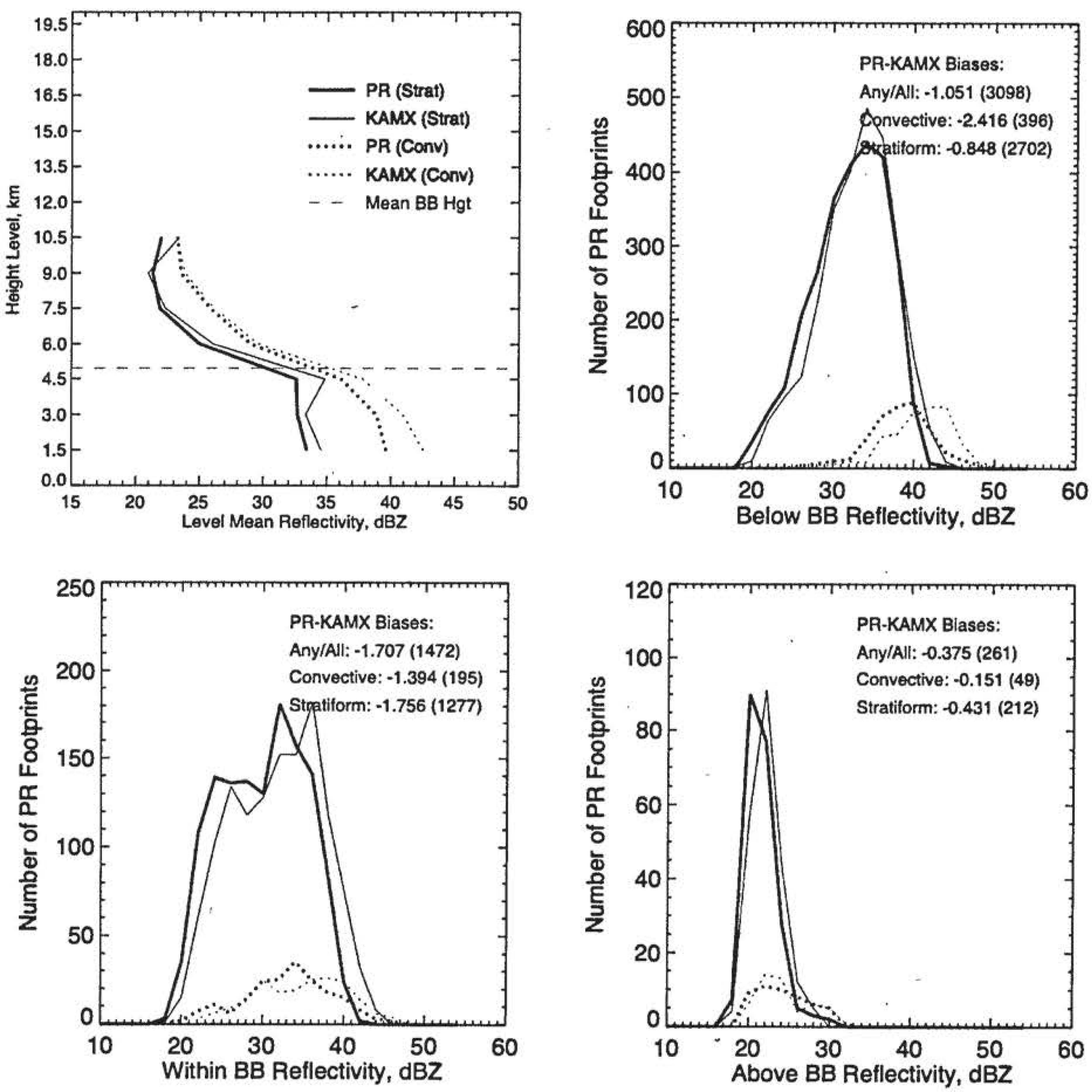

Figure 7. Vertical profile (upper left panel) and histograms of geometrically-matched PR (heavy lines) and GR (narrow lines) reflectivity samples for the case shown in Figure 6. Stratiform (convective) rain type is plotted as solid (dotted) lines. Separate histograms are plotted for sample points below (upper right), within (lower left) and above (upper right) the bright band. Vertical scale varies in the histograms. PR-GR mean differences (bias, in dBZ) and sample sizes, by rain type, are indicated for the data in each histogram. Histogram bin width for accumulations is 2 dBZ. Points are limited to where at least 95% of the gates averaged to produce the PR and GR match-up samples are above fixed thresholds (see Fig. 6 and text). Dashed horizontal line in the vertical profile indicates the mean bright band height as analyzed in the TRMM PR 2A-25 product.

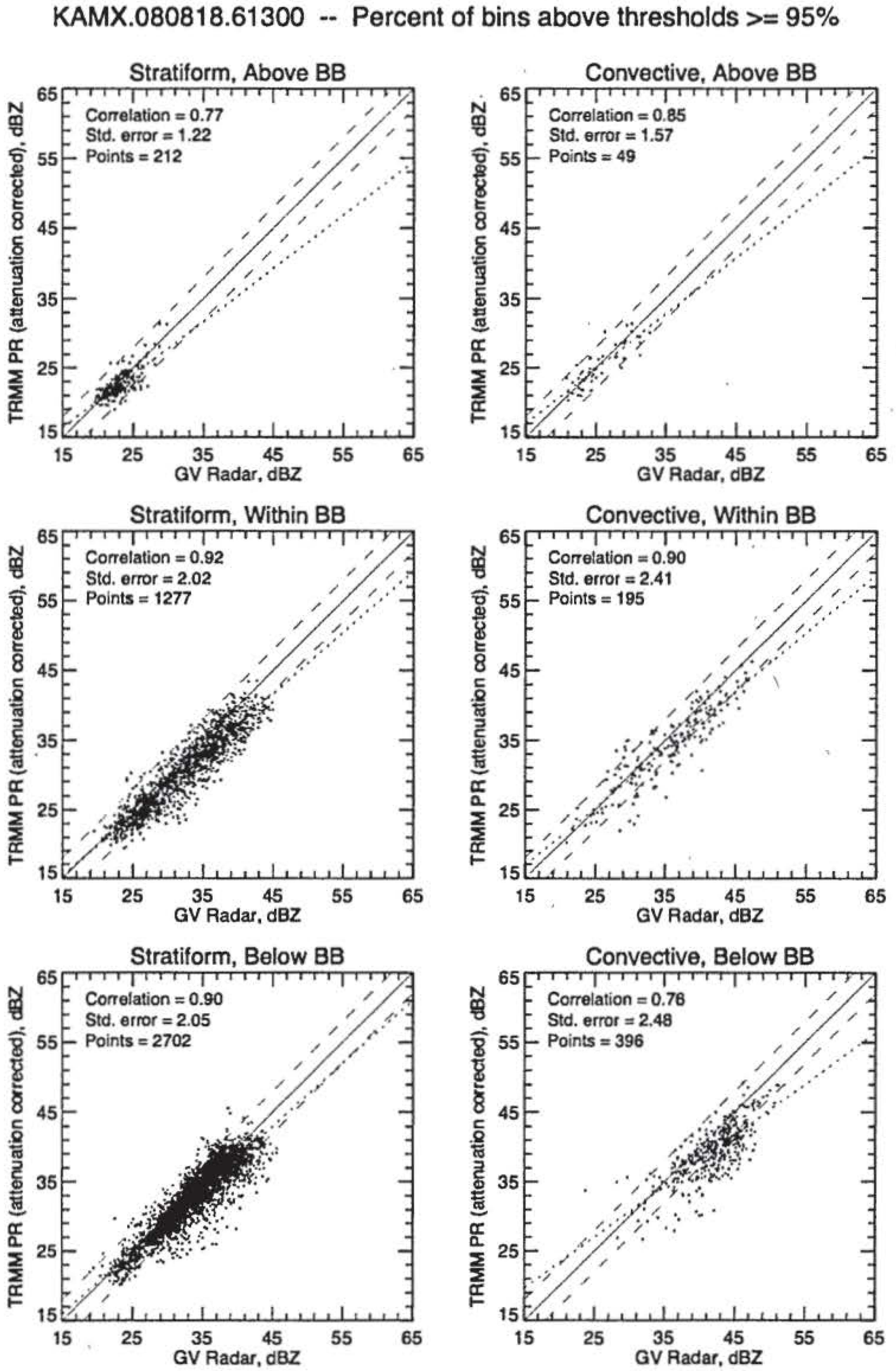

Figure 8. Scatter plots of PR vs. GR reflectivity for the same case and data constraints shown in Figs. 6 and 7. Solid lines indicate the 1:1 match, dashed lines indicate +/- 3 dBZ bounds, and dotted lines are the linear fit to the data.

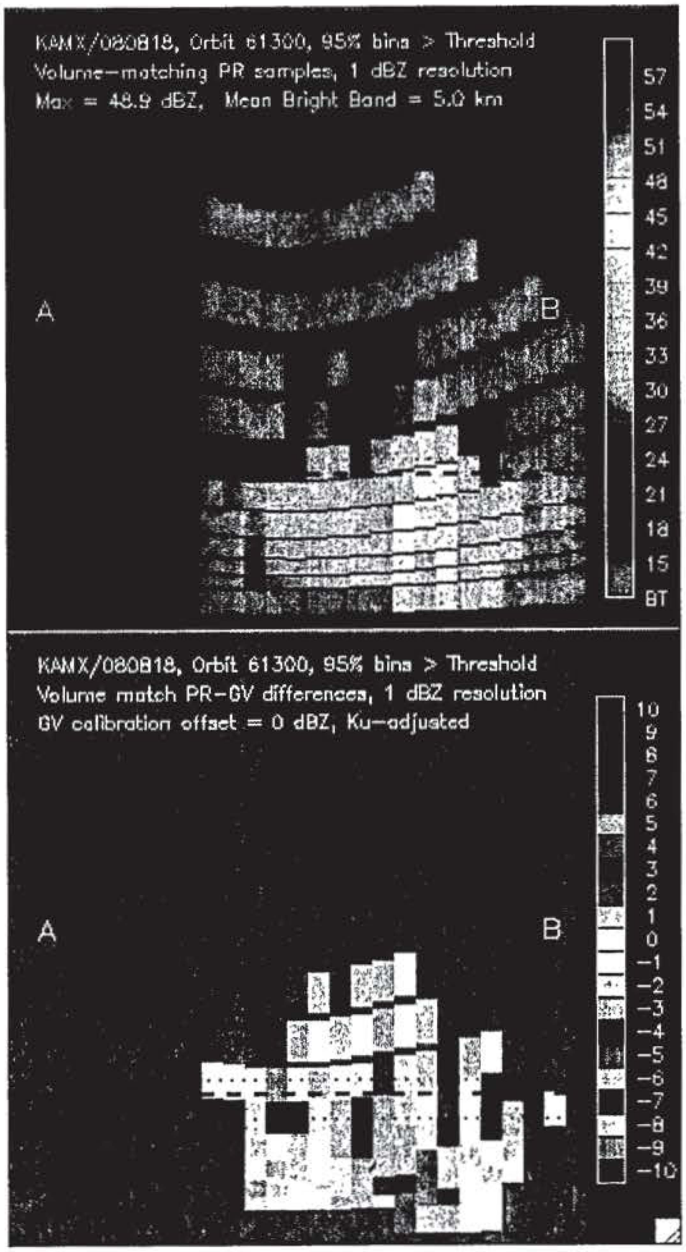

Figure 9. Vertical cross section, from 0-20 km height, of PR reflectivity (top) and PR-GR reflectivity difference (bottom) from geometrically-matched PR and GR data along the PR scan line labeled A-B in Fig. 6. GR data have had S-to-Ku band adjustments applied. PR data shown in gray show sample points rejected based on the threshold criteria of Fig. 6. Vertical extent of samples in the lower elevation sweeps has been adjusted to eliminate overlaps in the plots. The heavy dashed line indicates the mean bright band height, and dotted lines plotted 500 m above and 750 m below this height indicate the area of influence of the bright band (see text).

Site ID	Site name	Latitude deg. N	Longitude deg. E
KAMX	Miami, FL	25.6111	-80.4128
KBMX	Birmingham, AL	33.1722	-86.7697
KBRO	Brownsville, TX	25.9161	-97.4189
KBYX	Key West, FL	24.5975	-81.7031
KCLX	Charleston, SC	32.6556	-81.0422
KCRP	Corpus Christi, TX	27.7842	-97.5111
KDGX	Jackson, MS	32.3178	-89.9842
KEVX	Eglin AFB, FL	30.5644	-85.9214
KFWS	Dallas-Ft Worth, TX	32.5731	-97.3031
KGRK	Fort Hood, TX	30.7219	-97.3831
KHGX	Houston, TX	29.4719	-95.0792
KHTX	Huntsville, AL	34.9306	-86.0833
KJAX	Jacksonville, FL	30.4847	-81.7019
KJGX	Robins AFB, GA	32.6753	-83.3511
KLCH	Lake Charles, LA	30.1253	-93.2158
KLIX	Slidell, LA	30.3367	-89.8256
KMLB	Melbourne, Florida	28.1133	-80.6542
KMOB	Mobile, AL	30.6794	-88.2397
KSHV	Shreveport, LA	32.4508	-93.8414
KTBW	Tampa Bay, FL	27.7056	-82.4017
KTLH	Tallahassee, FL	30.3975	-84.3289
RGSN	*Gosan, Korea*	*33.2942*	*126.1630*
RMOR	*ARMOR, Huntsville*	*34.6460*	*-86.7700*
DARW	*Darwin*	*-12.2522*	*131.0430*
KWAJ	*Kwajalein atoll*	*8.7180*	*167.7330*

Table 1. Ground radar sites included in the current GPM GVS Validation Network.

Table 2
TRMM Precipitation Radar Reflectivity Factor Bias Compared
to WSR-88D Ground Radars. Values for μ and σ in dBZ.

	Convective	Stratiform
Above BB	$\mu=0.298$, $\sigma=3.94$ ($\mu=-0.993$, $\sigma=4.24$) n=3,850	$\mu=-0.0975$, $\sigma=1.79$ ($\mu=-0.629$, $\sigma=1.91$) n=7,207
Within BB	($\mu=-0.542$, $\sigma=4.88$) n=896	($\mu=-2.60$, $\sigma=3.91$) n=13,646
Below BB	$\mu=-1.42$, $\sigma=4.15$ ($\mu=0.433$, $\sigma=3.95$) n=5,618	$\mu=-1.01$, $\sigma=2.77$ ($\mu=-0.120$, $\sigma=2.66$) n=37,477

Table 2. Mean, μ, and standard deviation, σ, of Precipitation Radar (PR) instrument bias compared to WSR-88D Ground Radar (GR) measurements for samples from above, within, and below the melting layer (bright band, BB). The bias was calculated as PR minus GR reflectivity factor for match-up samples. Bias estimates are based on the use of GR data corrected as described in the text; results using uncorrected GR data are in parentheses. The sample size, n, is identified for each case.

Table 3
TRMM Precipitation Radar Reflectivity Factor Bias Compared
to individual WSR-88D Ground Radars,
for Stratiform Rain Samples Above the Bright Band.

Radar ID	PR-GR_{Ku} Mean Difference (dBZ)	PR-GR Mean Difference (dBZ)	PR Mean Reflectivity (dBZ)	Ku-Adjusted GR Mean Reflectivity (GR_{Ku}) (dBZ)	GR Mean Reflectivity (dBZ)	Total Samples
KAMX	0.03	-0.49	22.65	22.63	23.14	2304
KBMX	-0.77	-1.47	23.9	24.67	25.37	12194
KBRO	-0.51	-1.12	23.15	23.66	24.27	2009
KBYX	0.04	-0.49	22.77	22.74	23.26	1042
KCLX	-0.76	-1.42	23.54	24.3	24.96	9071
KCRP	0.51	-0.03	23.37	22.86	23.39	2808
KDGX	0.07	-0.53	23.65	23.58	24.18	7266
KEVX	-0.07	-0.68	23.61	23.68	24.29	6488
KFWS	0.97	0.43	23.78	22.81	23.35	11910
KGRK	2.63	2.19	24.19	21.55	21.99	6871
KHGX	-0.09	-0.68	23.46	23.54	24.14	3332
KHTX	0.44	-0.16	23.96	23.52	24.12	12141
KJAX	-0.72	-1.33	22.95	23.68	24.29	4509
KJGX	0.73	0.17	23.81	23.09	23.65	6569
KLCH	-1.34	-2.06	23.54	24.89	25.6	4071
KLIX	-1.46	-2.15	23.18	24.64	25.33	7955
KMLB	0.71	0.26	22.52	21.81	22.27	2787
KMOB	1	0.5	23.37	22.37	22.87	4772
KSHV	-1.04	-1.71	23.35	24.39	25.06	8000
KTBW	-0.98	-1.62	22.99	23.97	24.61	3309
KTLH	-1.62	-2.34	23.37	24.99	25.71	3280

Table 3. Mean Precipitation Radar (PR) instrument bias compared to WSR-88D Ground Radar (GR) measurements for samples from above the melting layer, by GR site. The bias was calculated as PR minus GR reflectivity factor for match-up samples. Bias estimates are shown for both frequency-corrected GR data (GR_{Ku}) and uncorrected GR data. The sample size is identified for each site.

Height (km)	Any Type		Stratiform		Convective		PR max reflectivity (dBZ)	GR max reflectivity (dBZ)
	PR Bias	Total	PR Bias	Total	PR Bias	Total		
1.5	-1.341	1251	-1.110	1096	-2.902	155	48.949	50.952
3.0	-0.828	1502	-0.650	1313	-2.053	189	46.439	50.640
4.5*	-2.162	990	-2.229	868	-1.695	122	45.684	46.522
6.0	-0.963	497	-1.041	415	-0.584	82	41.137	42.111
7.5	-0.400	81	-0.428	63	-0.313	18	30.208	32.672
9.0	0.037	12	0.384	6	-0.304	6	25.007	28.599
10.5	-0.654	2	-1.394	1	0.072	1	23.253	23.392

Table 4. Vertical profile of PR-GR mean reflectivity difference (bias) and maximum PR and GR sample reflectivity for the case shown in Figs.6 and 7. The asterisk at 4.5 km indicates the level under the influence of the bright band.